

SALT WEATHERING OF IMNI TOMB. PROBLEM IDENTIFICATION AND CHARACTERIZATION

Shaaban ABDELAAL^{1*}, Randa YAMANI²,
Mostafa ABDEL-FATAH³, Ioan Gabriel SANDU^{4,5}

¹ Fayoum University, Faculty of Archaeology, Restoration Department, Egypt.

² National Institute of Standards, Reference Materials Department, Giza, Egypt

³ Egyptian Ministry of Archaeology, Egypt

⁴ Gheorghe Asachi Technical University of Iasi, Materials Science and Engineering Faculty,
53A D. Mangeron Blvd., 700050 Iasi, Romania

⁵ Romanian Inventors Forum, 3 Sf. Petru Movila St., Bloc L11, III/3, 700089 Iasi, Romania

Abstract

Imni Tomb is one of the most important tombs in Lisht, which was called Ist tawy in ancient Egyptian language. It is located about 60 km south west of the Egyptian capital Cairo, its history dating back to the Middle Kingdom that included two phases, the 11th Dynasty and the 12th Dynasty between 2050 to 1710 B.C. El-Lisht was investigated in 1882 by Egyptologist Gaston Maspero. The tomb suffered from salt weathering. The salt crystals can be seen clearly and starkly in the form of thick crust on the exposed surface of the tomb limestone and on the painted inscriptions. It led to losing some inscriptions and damaging others. Crystallized salts appeared in several forms; fluffy, needle, prismatic and cubic form. This proposal aimed to study the action of salts in Imni tomb, through studying the types of salts, the building materials and the nature of bed rock surrounding the tomb. types of salts formed were investigated to identify their origin, source and the crystallization process as well as studying the quality of building materials in the tomb, the bedrock to see the impact of salt weathering on them, and to determine the root causes of the problem and to develop a proposal for treatment and conservation. This study was carried out by using a variety of methods of analysis and examination. Physical properties of the building materials of Tomb. Generally, the results indicated that Calcite (CaCO_3) was the main component of the Imni tomb and Halite (NaCl) was the main crystalized salt on the surface. The main source of these salts is the mother rock, where the salts are present in abundance and density. Salts crystallization in-between the minerals grains or below the exterior surface was the main cause of deterioration the exterior polish surface of the limestone blocks and what they had of painted inscriptions.

Keywords: Egypt; El-Lisht.; Imni Tomb; Salt weathering; XRD; XRF; Polarizing Microscopy.

Introduction

Al-Lisht archaeological region is located 60km south west of Cairo, Egypt. It is considered one of the most important archaeological sites in Memphis cemetery, as it was a central place for the eleventh and twelfth dynasties that dated back to the era between 2050 and 1070 B.C. [1-2]. The region contained many tombs of pharaonic age, which are distinguished and very important such as Senosert Ankh and Imenimhat tombs [3-4]. The most important one is the tomb of Imni "the leader of the army" (Fig. 1), which was discovered in 1882 by Gaston Maspero [5-6].

* Corresponding author: smm00@fayoum.edu.eg

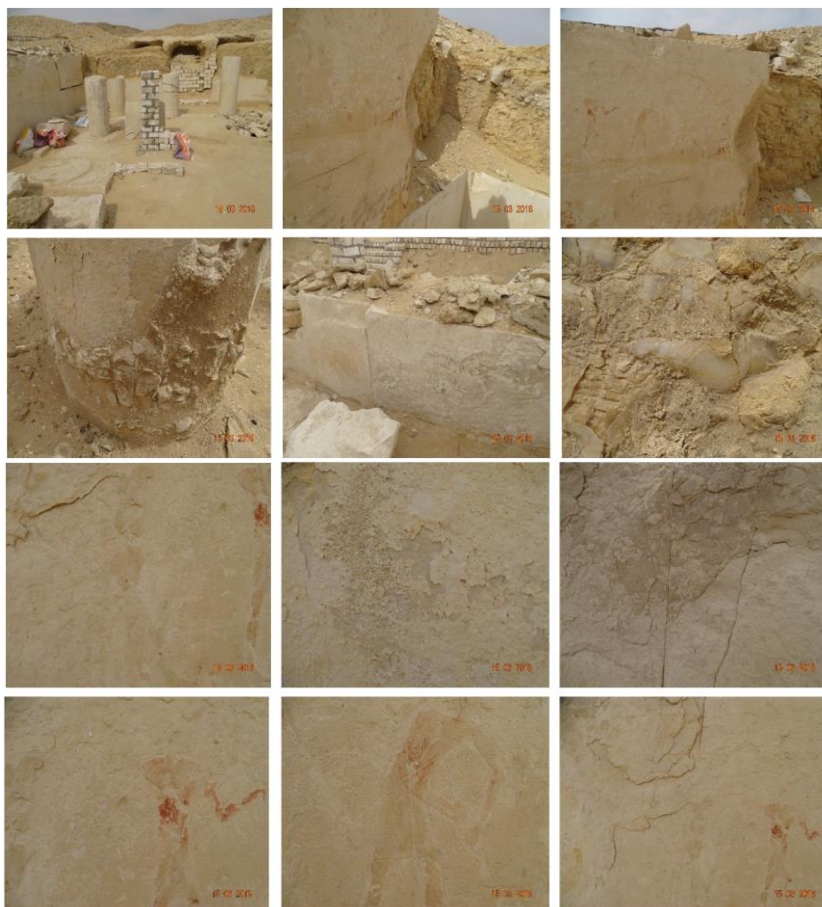


Fig. 1. Parts of the tomb which indicated the salt weathering for painted inscriptions and building limestone

Salt weathering is considered one of the most fatal deterioration factors which damage the building materials and the exposed bed rock. A lot of researches focused on that factor because many of ancient Egyptian archaeological buildings such as tombs and temples decayed and deteriorated because of it [7-9].

The past decennium has seen a growing scientific concern in the still poorly understood subject of salt weathering, a phenomenon with considerable cultural and economic results. This interest has led to an accretion in research and growing clearness of the roles of salts in weathering and destruction [10].

Salt weathering is a major decay mechanism affecting historic architecture and statuary, as well as archaeological tombs. Many archaeological sites in Egypt in general, suffered from severe deterioration factors compared to the conditions in which they were originally discovered and excavated, as the absence of durable conservation practice, exposure to semi-arid climatic conditions, increasing pollution and pressure. Rock porosity influences permeability and makes space for water retention. Many archaeological tombs in Egypt have already been partially or even completely destroyed by salt attack. The most common and dangerous salts present in Egyptian stone buildings was sodium chloride in the form of Halite (NaCl), and gypsum [11-13]. The most dangerous ones are often highly soluble in water that transported within the porous material by physical processes such as crystallization pressure

process. Salt damage of building stones are normally associated with the variation of the water content of the porous material as well as the humidity fluctuations of the surrounding environment. As a result, salt phase transitions and crystallization will appear. It is known that, the air pollution, ground water rising up through foundations and the use of inappropriate treatments materials are the main sources of the salts in addition to building materials which may carry salts as a natural component in their composition [14-18].

The salts usually crystalized in three forms; on the exposed surface (efflorescence), between the different surfaces (sub-florescence) and inside the material pores (crypto-florescence) [19-22]. The location of salt crystallization depends on the flow of water and the permeability of the substrate, which allows the salt to move. The crystallization of salt causes a rise in volume and the thermal expansion differences between the salts and building material lead to internal stress. The salt liquid phase permits salts to be transported and evaporated which can occur on the exposed surfaces (efflorescence) or in the pores (crypto-florescence) [23-26]. The deterioration effect caused by the salt strongly depended on the nature of the building material and the surrounding environmental conditions. In the semi-arid environment, which characterized by its extreme climate and the diverse of temperature and humidity in addition to the condensation which occurred in the first hours of the day leads to crystallization and dissolution of the salts in repeated actions. As a result, it leads to deform and crack the building material. During the recrystallization process, the cracks are enlarged and spalled the architectural elements such as pillars. Also, the availability of the salty solution and the fluctuation of air movement in the open area of the semi-arid environment lead to continuous crystallization of the salts on the external surface in the form of thick crust [27-31].

Some authors studied the crystallization process of soluble salts inside the natural porous of the materials which was partially immersed in different saline solutions. Porous materials are suitable for migration of salt solution to the surface, where salt can be crystallized [32-36].

The aim of the present work was to identify the type of salt causing the weathering of Imni Tomb. Various analytical techniques were used to investigate the formed phases and their crystal structure such as using X-Ray diffraction spectrometer (XRD), X-Ray Fluorescence spectrometer (XRF), Optical and polarized Microscope and (FTIR) Fourier Infra-red spectroscopy.

During the field visit of the tomb, as shown in the images in figure 1, it is clear that the tomb was built at the foot of the mountain, the stone blocks appeared to have different colors than the parent rock.

The tomb lost great part of their painted inscriptions because of the salt weathering on the surfaces of the walls of the tomb and its columns which was detected to the naked eye. These salts formed in many forms, shapes and colors. It threatened the inscriptions on the stones to be completely lost as shown in figures 2 and 3.

Materials and Methods

Sampling

Stone Samples

A number of stone samples were collected from the walls, the foundations and from the pillars of the tomb. Also, other samples were collected from the mother rock where the tomb was hewed and built to investigate the main components.

Salt Samples

During the field survey of the tomb of Imni, salt crystallization was detected. Those salts were crystallized on the walls of the tomb and above the painted parts and inscriptions. They took several forms on the walls of the tomb. The visual detection showed that, salts had various colors such as white, yellowish, and bluish white. Samples of salts were collected from different

locations of the walls of the tomb, from pillars and their foundations in addition to the bed rock. (Figs. 2, 3, 4 and 5)

Painted Samples

Although the tomb had some red painted places, red painted inscriptions are in very poor conditions due to the crystallization of salts on the surface of the walls. A red sample of painted inscription was collected as well to identify the pigment used and the organic binder too (Fig. 1).

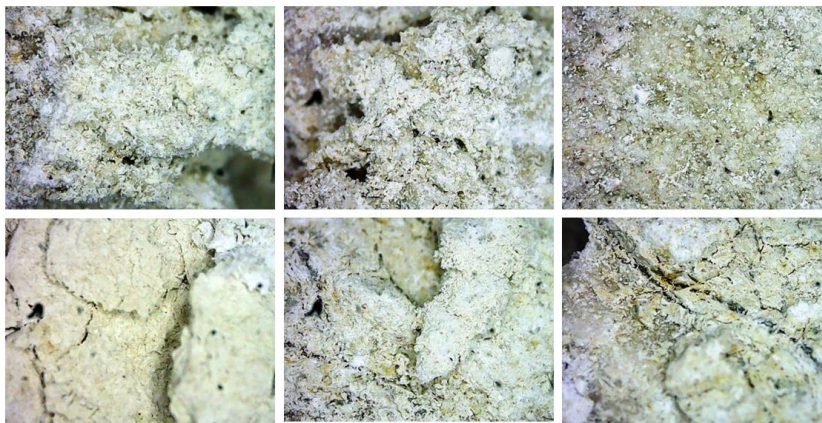


Fig. 2. Optical microscope investigation of lime stone building walls showed many fine cracks, empty in some cases filled with salts., salts covered most of the sample surface some gaps and cracks, weakness of the surface

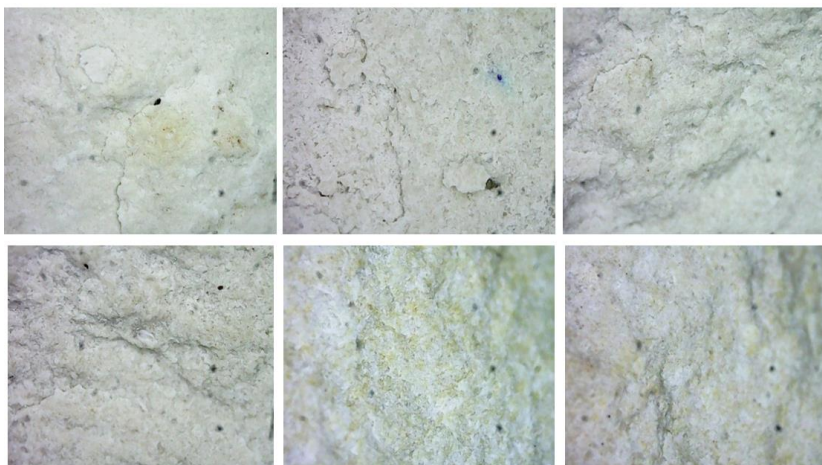


Fig. 3. The visual study with light microscope of samples of stone walls.
The samples showed cracks and decomposition of the surface and sample of the pillar

It is characterized by crystallization and recrystallization as a result of their hygroscopicity, causing pressure on the exposed surfaces of the stone structure. When the salts started to crystalize on the surface of the stone, it takes several forms such as fluffy, needle, prismatic and cubic. Therefore, the importance of this study is to determine the nature of salt weathering that hit the tomb, its inscriptions and the quality of crystallized salt, as well as studying the quality of the building stone, its nature and its characteristics to show the extent damage which hit the tomb and find out the most appropriate treatment and protection methods (Figs. 4, 5 and 6).

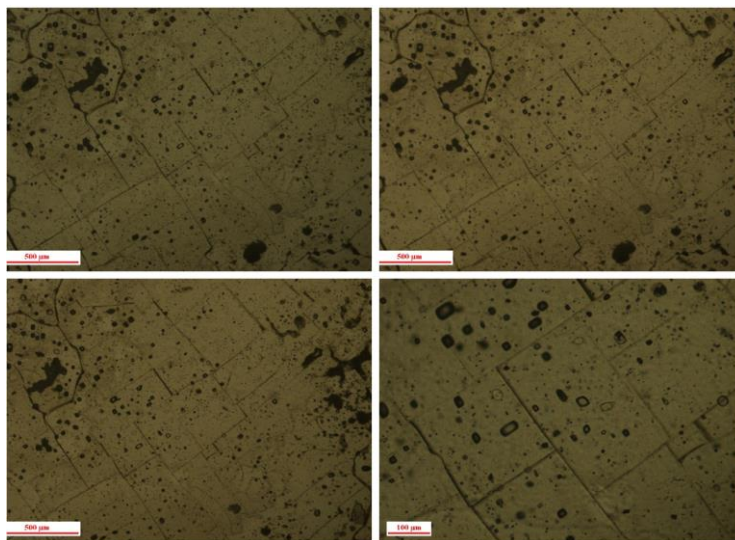


Fig. 4. Polarizing microscope investigations of salts samples which indicated the full crystallization of salts that taken a cubic shape

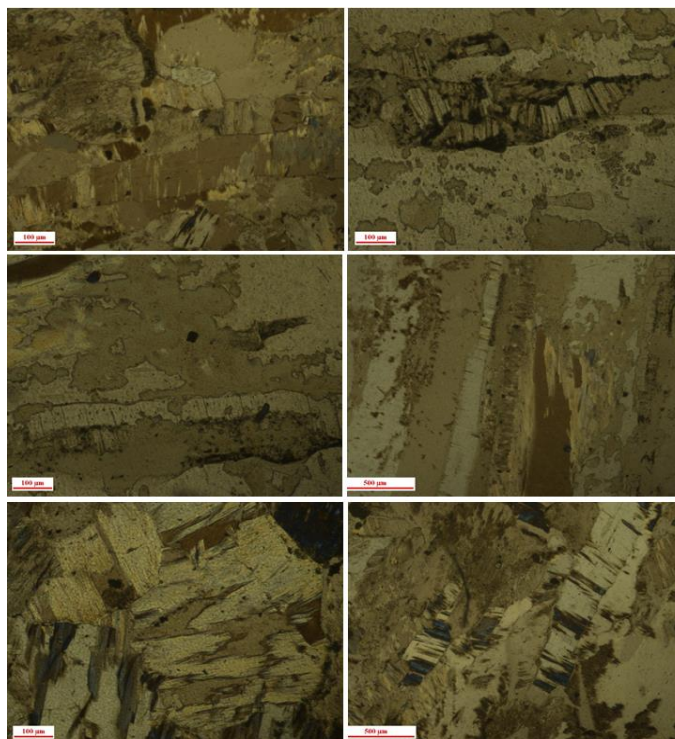


Fig. 5. Polarizing microscope examinations of salts samples taken from places less exposed to sunlight. Salts looks like saline veins overlapping with the limestone structure, causing saline breaks to weaken the stone construction

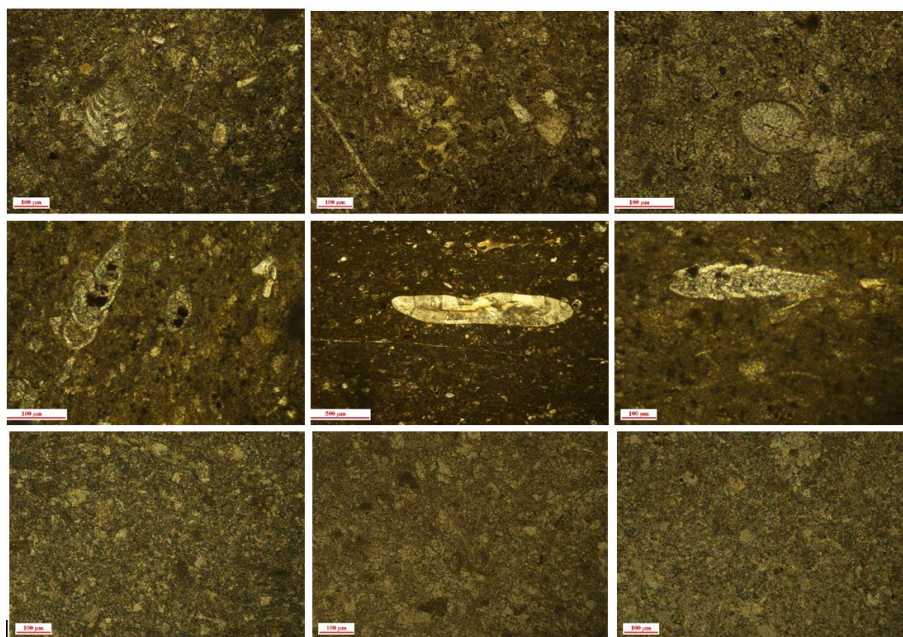


Fig. 6. The photographs with Polarizing Microscope showed that, fossils and organic remains were found in the limestone samples used in the walls, columns and bases of the tomb. Indicating that the limestone used on walls of the tomb is dolomite As for the samples of the mother rock, it is clear from the three pictures in bottom that there are no organic remains

Instruments and Analytical methods

Microscopy Examination

The samples were investigated and studied by using the Wild M8 stereomicroscope, with the Olympus BX51 optical microscope [37-39].

Polarized Microscope was used to investigate and examine the samples which prepared for that purpose. Samples were prepared in Faculty of science department of geology, Cairo University for a thin section mode. Four stone samples were prepared on glass thin section in dry mode. Two of them were from adding stone and others from bed rock (mother rock surrounding the tomb). Four salts sample were collected from fabricated stones and the bed rock [40-42].

Fourier transforms infrared spectroscopy (FTIR)

One sample from red painted inscriptions was prepared and analyzed by FTIR (infrared absorption transmission method), Perkin Elmer Spectrum, USA to identify the organic medium which was used in painted inscriptions. The measurement was done in the range between 4000-400 cm^{-1} to identify the organic functional groups presents in red painted sample and to classify the type of organic binder that used in painted process [43-50].

XRD measurements

Phase identification and crystal structure were investigated using XRD spectrometer, Panalytical, the Netherlands, Eperyam model, Cu anode at $\lambda = 1.54\text{nm}$ with fixed slit module. The samples were manually grinded to powder form and analyzed with 2Θ range from 5° to 90° with step size of 0.013 and 30sec/step [51-55].

XRF measurements

Elemental analysis was done using XRF, Axios model from Panalytical, the Netherlands. The samples were prepared in pressed tablets. 9g of samples were mixed with 2g of wax materials which acts as a binder for pressing. The mixture was pressed at 50KN for 10 seconds in aluminum dish prior to analysis [56-58].

Total dissolved solids (T.D.S)

The T.D.S device is used to identify the total dissolved salts ratio in solutions (the device was used in this process records from 1 to 1990ppm). The sample was prepared by grinding it to powder to pass from 425 μ m (micrometer) sieve, then adding 2g of this powder to 100mL of water and stirred well then left for 24 hours and T.D.S value was identified. The T.D.S ratio was calculated according to the following formula [59-61]:

$$\text{Salts (\%)} = (\text{T.D.S of sample in water/weight of the sample (mg)} \\ \times \text{water quantity used/1000mL}) \times 100$$

Physical properties

Visual investigation by naked eye. The samples of the tomb consisted of two groups, the first group represented the samples of mother rock and the second group represented the samples of the stones used as building materials in the tomb. The first type consisted of yellow rocks but in different layers with different thickness and its color changed little from yellow to light yellow. All the mother rock layers in the tomb were covered with thick layer of salts which formed a protective layer to the external surface of the rocks so this layer helped the rocks to resist the weathering process however the salts in the first stages of crystalized caused fine cracks which contributed in weaken the external surface of the rocks.

The bulk density. The samples densities were identified by using the two weights method. The sample was dried for 48h at 105°C in drying oven and was weighted by sensitive balance to the nearest 0.01g then the sample was immersed in water for 24h then weighted suspended in the water. The density was determined according to the formula [62]:

$$D \text{ bulk (g/cm}^3\text{)} = W_{\text{dry}}/W_{\text{sus}},$$

where: W_{dry} = the weight of the dried sample in the air; W_{sus} = the weight of the sample suspended in water.

The porosity. The porosity of the samples is important to determine the behavior of rock with different factors. The resistance of material to deterioration process depends on many factors; the porosity is the most important one. The porosity depends on the conditions of formation, the site of the samples in addition to the chemical composition. There is a relation between porosity and density. The porosity in general can be determined by the relation between the weight of water absorbed to the volume of the sample or by the relation between the density of the material and the particle density subtracted from one [63]:

$$\Phi = ((W_{\text{sat}} - W_{\text{dry}})/W_{\text{sus}}) \times 100 \\ \text{Or } \Phi = 1 - (D \text{ bulk}/D \text{ particle}) \times 100,$$

where: W_{air} = the weight of the dried sample in the air; W_{sat} = the weight of the saturated sample with water; W_{sus} = the weight of the suspended sample in water.

The natural water content (NWC). Three samples of every type of rocks and stones were tested to determine the natural water content by using the two weights method. The weight of sample in the air was identified, then the sample dried in an oven for 48 hours at 105°C, then weighted again. The NWC was determined by using the following formula [64]:

$$\text{NWC (\%)} = (W_{\text{air}} - W_{\text{dry}}/W_{\text{dry}}) \times 100$$

Water Absorption (WA). Three samples of every type were tested to investigate their ability to absorb water. The two weights methods were used to measure the values of WA. The weight of the dried sample in air was recorded then the sample weighted after soaking in water for 48 hours. WA was calculated according to the following formula [65]:

$$WA = (W_{\text{sat}} - W_{\text{dry}}/W_{\text{dry}}) \times 100.$$

A.I.R Test. This test aimed to identify the ratio of soluble and insoluble components whereas carbonate (calcite minerals in the rocks and stones) reacts with HCl to produce CaCl_2 which is soluble in water according to the formula:



while the quartz, clay minerals and salts do not react with HCl so they stay as insoluble materials which can be identified by weighing after filtering and drying [65].

Compressive Strength. Non-destructive Schmidt Hammer test of type N was used to identify the compressive strength of the rocks and stones. The rebound values are displayed on a mechanical sliding scale then according to the table on the Schmidt hammer it can be changed into N/mm^2 and then to Kg/cm^2 [65].

Surficial Moisture monitoring. Hydromette Compact B.Th. Compact B was used to measure the surficial Moisture. It is an electronic structural moisture indicator based on a non-destructive dielectric constant measurement or high frequency measuring method.

Temperature monitoring. The Wohler HYGROTEMP 24 (6603) Non-Contact Temperature and Humidity Meter was used to measure the temperature.

Results

Light Optical Microscope

The visual tests were carried out in the field for the stones which were used in the construction of the architectural elements of the tomb showed some important indications about the nature of the building material and its current condition, state and the extent of damage and deterioration as in figures 2 and 3. The results of the optical microscope showed the weakness of exterior surface of the limestone, a number of cracks, the large bloom and crystallization of salts. The yellow layered limestone affected by touch and decomposed in water in short time. Fine cracks, empty ones and in some cases filled with salts. The salts covered most of exposed surface of the samples with some gaps and cracks.

Polarizing Microscope

The investigation by using polarized microscope of the limestone samples used in the construction of the walls of the tomb presented in figure 6 confirmed that, the results received from the light microscopy investigation. Also, some fossils and organic residues were presented in a large and intensive manner, which took various forms, including plant, animal and other forms. These results revealed that, limestone was used as a building material and quality limestone, reflecting that, limestone was not used from the surrounding environment in the construction of the tomb. The results revealed that, there were no fossils or organic materials in the mother rock but confirms the presence of salts. Samples of salts prepared for polarized microscopy examination showed that, Samples of salts taken from the sun's bright side of the tomb were completely crystallized which revealed that, the salts completed all stages of crystallization and formed a cubic shape in a perfect method which indicated that samples were taken from sunny places (Figs. 4 and 5). They looked like veins overlapping with the limestone structure, causing breaks the stone construction.

FTIR of organic medium Results

Through the analysis of the pattern of infrared absorption of the red colored archeological sample and compared with the standard media that commonly used in the Egyptian coloring as gum Arabic, animal glue and egg yolk. The FTIR results in figure 7 showed that, Arabic gum was the organic medium used for the inscriptions paintings in the tomb of Imni in the Lisht area.

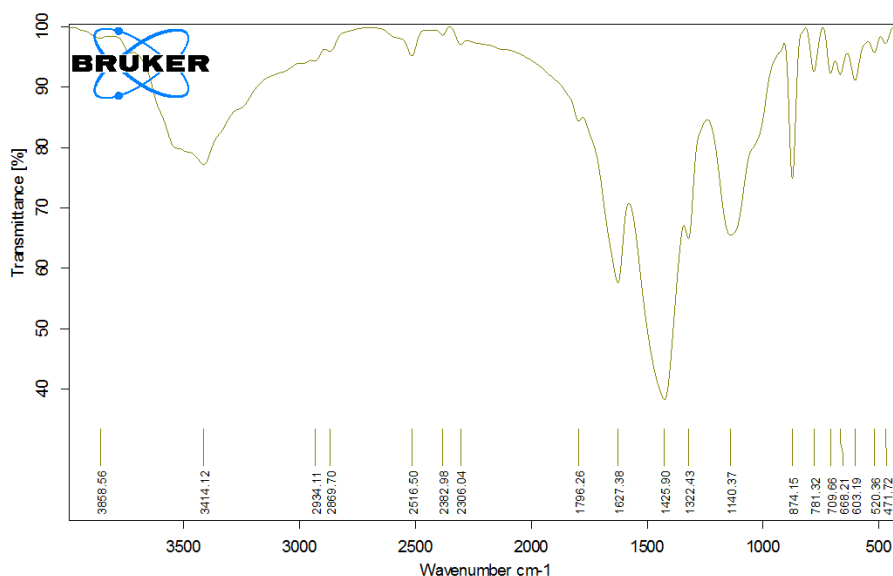


Fig. 7. FTIR pattern of red painted archaeological sample indicated Arabic gum was used as organic binder in painted inscription.

XRD measurements

Mother rock samples

The X-ray diffractograms illustrated in figure 8 of mother rock sample indicates the characteristic peaks of calcite phase (CaCO_3) which was the major phase and the main component of the mother rock. The structure of calcite at room temperature is rhombohedral (space group R3c).

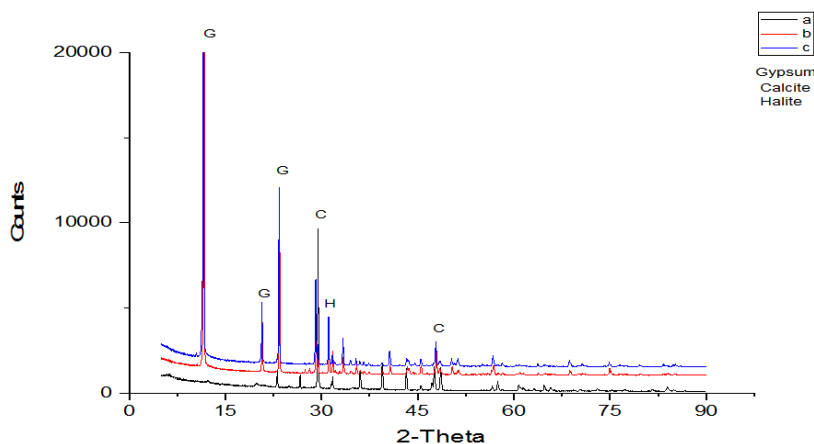


Fig. 8. X-ray diffractogram of mother rock and the salt formed

Also, gypsum phase was indicated in the diffractogram of the mother rock as illustrated in figure 9. Gypsum (calcium sulfate dihydrate) is a monoclinic system consists of layers of SO_4^{2-} tetrahedral bound together by Ca^{2+} cations. Gypsum is also considered as a deteriorating agent. Gypsum crystals may be formed due to the direct crystallization with the fairly constant supply of moisture or due to the reaction of air pollution with the calcareous materials.

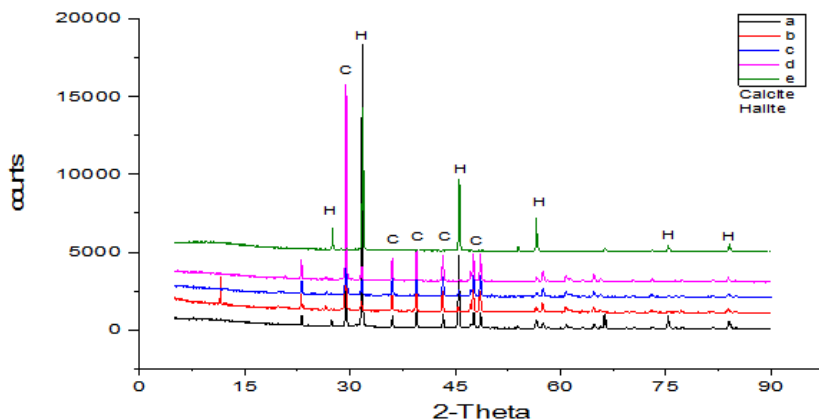


Fig. 9. X-ray diffractogram of mother rock (a,b) and gypsum (c)

Salt samples from mother rock

Halite phase also indicated in the x-ray diffractogram in large quantities inside the mother rock, figure 10. The crystal structure of halite is the cubic system with a face centered lattice, f.c.c. (space group Fm3m) with a two-atom basis or as two interpenetrating face centered cubic lattices. The first atom is located at each lattice point, and the second atom is located halfway between lattice points along the fcc unit cell edge. Halite is one of the most compounds causes deterioration of porous materials with the aid of the environmental conditions like pressure, temperature and moisture.

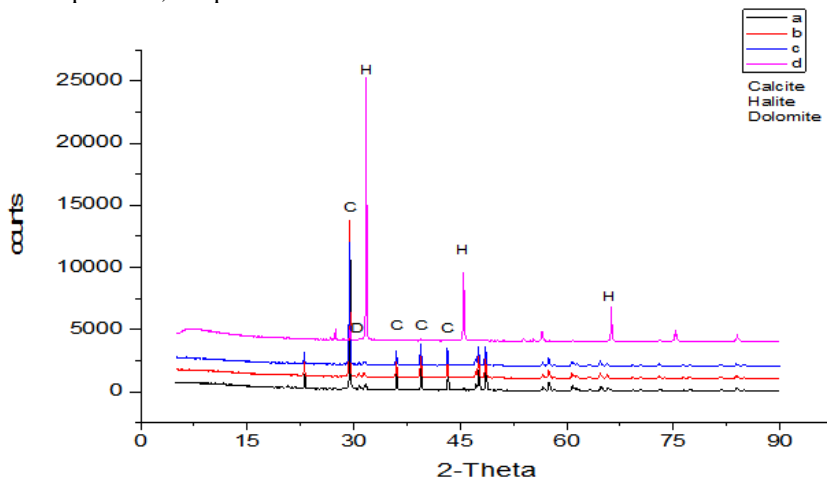


Fig. 10. X-ray diffractogram of east wall of the tomb (a, b, c, d) and the salt formed (e)

Tomb stone samples

On the other hand, X-ray diffractograms from different corners of the tomb and the pillars illustrates the characteristic peaks of the calcite phase with small amounts of halite which may be transferred to the tomb pillars as shown in figures 11, 12, 13 and 14. The strength of white stones which were used in building the tomb such as walls, pillars and foundations recorded higher values of C.S than the mother rock. And this because of Dolomite whereas X-ray phase analysis indicated the presence of dolomite phase which is harder than calcite in the white limestone samples. Dolomite (double carbonate of calcium and magnesium $\text{MgCa}(\text{CO}_3)_2$) crystallizes in the trigonal-rhombohedral system (space group R-3).

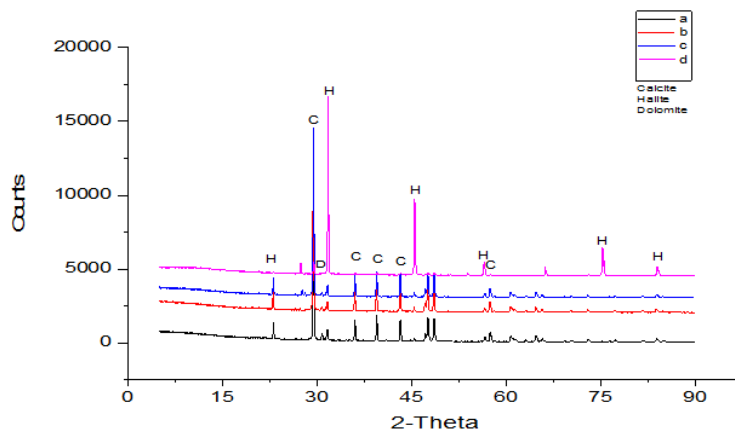


Fig. 11. X-ray diffractogram of west wall of the tomb (a, b, c) and the salt formed (d)

Tomb salts samples

XRD analysis results of all salts which crystalized on the surfaces of the four walls of Imni tomb indicated that, the salt was Sodium Chloride in the form of halite (NaCl).

Pigments sample

The main and the only pigment was used in the tomb is red pigment and XRD analysis results in figure 15 indicated that, Hematite (Iron Oxide, Fe_2O_3) was the main material which used for red painting inscriptions in the tomb.

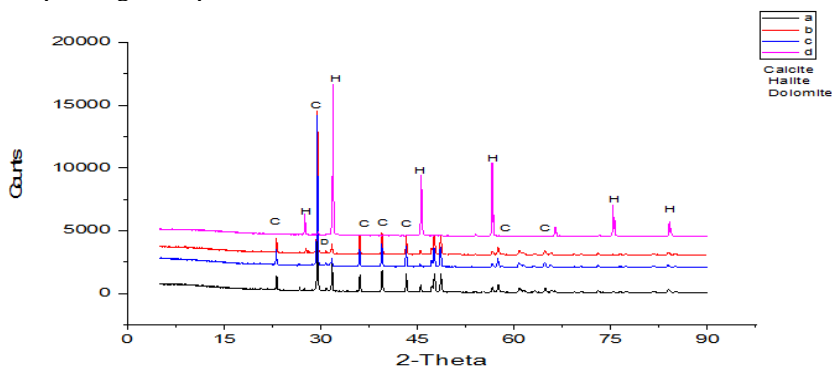


Fig. 12. X-ray diffractogram of north wall of the tomb (a, b, c) and the salt formed (d)

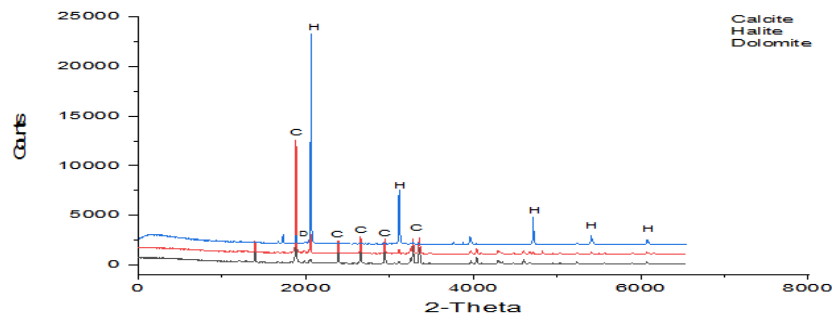


Fig.13. X-ray diffractogram of south wall of the tomb (a, b, c) and the salt formed (d)

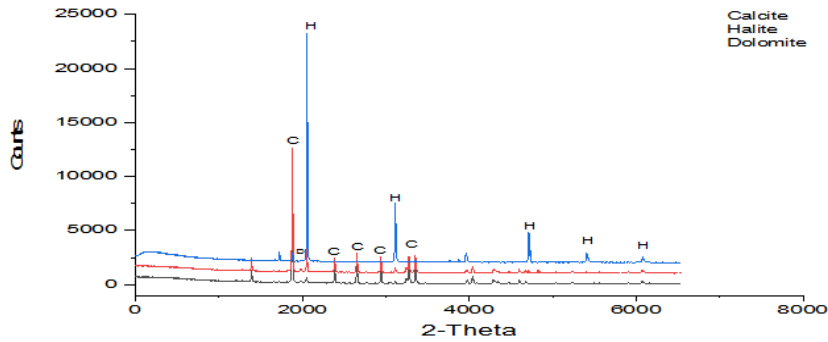


Fig. 14. X-ray diffractogram of tomb column (a, b) and the salt formed (d)

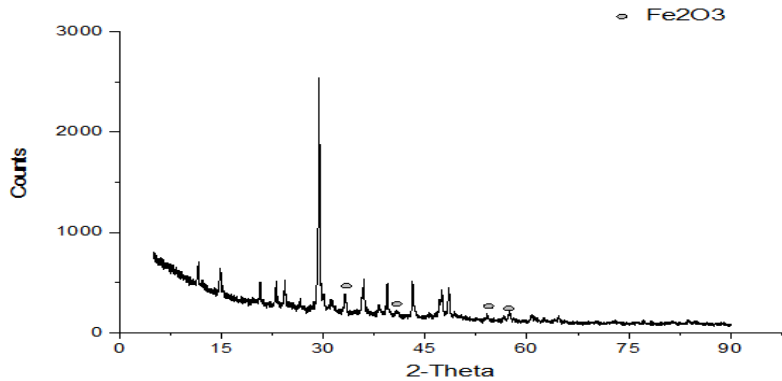


Fig. 15. X-ray diffractogram of the pigment sample

XRF measurement results

Salts samples

XRF analysis results illustrated in table 1 for the salts which crystalized on the surfaces of all the four walls was Halite sodium chloride NaCl, and the same results for the mother rock salts plus Gypsum which found in the mother rock as Gypsum veins.

Table. 1. Chemical composition of salt samples collected from the mother rock

| Element | S1 | S2 | S3 | S4 | S5 |
|---------|--------|--------|--------|--------|--------|
| O | 15.163 | 25.565 | 31.323 | 17.223 | 15.163 |
| Na | 16.848 | 9.438 | 0.501 | 15.703 | 16.848 |
| Mg | 0.044 | 0.239 | 0.352 | 00.109 | 0.044 |
| Al | 0.249 | 1.259 | 1.592 | 0.509 | 0.249 |
| Si | 0.528 | 2.738 | 3.573 | 1.129 | 0.528 |
| P | 0.011 | 0.050 | 0.073 | 0.020 | 0.011 |
| S | 0.121 | 0.090 | 19.50 | 0.364 | 0.121 |
| Cl | 58.647 | 24.397 | 1.926 | 49.607 | 58.647 |
| K | 0.061 | 0.238 | 0.374 | 0.121 | 0.061 |
| Ca | 7.948 | 33.375 | 23.3 | 14.407 | 7.948 |
| Ti | 0.031 | 0.164 | 0.402 | 0.062 | 0.031 |
| Fe | 0.325 | 2.225 | 5.44 | 0.686 | 0.325 |
| Sr | 0.023 | 0.179 | 0.649 | 0.060 | 0.023 |

Stone samples

XRF quantitative analysis in table 2 was carried out for the stone samples from the four walls of the tomb, the results confirm that, calcite was the main component for the walls due to the presence of large amount of calcium and oxygen according to table 1 plus dolomite, and the same one for column and its bases.

Table. 2. Chemical composition of different samples taken from the tomb corners

| Element | ST1 | ST2 | ST3 |
|---------|--------|--------|--------|
| O | 15.090 | 14.200 | 16.098 |
| Na | 1.534 | 0.096 | 0.175 |
| Mg | 0.224 | 0.117 | 0.178 |
| Al | 0.435 | 0.255 | 0.836 |
| Si | 1.073 | 0.579 | 1.800 |
| P | 0.001 | 0.030 | 0.053 |
| S | 0.042 | 0.037 | 0.025 |
| Cl | 0.599 | 0.363 | 0.463 |
| K | 0.144 | 0.061 | 0.107 |
| Ca | 29.4 | 25.785 | 24.852 |
| Ti | 0.000 | 0.047 | 0.138 |
| Fe | 2.872 | 0.945 | 2.235 |
| Sr | 0.201 | 0.279 | 0.310 |

TDS results*Limestone of the mother rock and white wall*

The results showed that, all the weathered samples contained different ratios of T.D.S according to their chemical composition and their physical properties. From table 3, the yellow weak samples showed the lowest ratio while the hard sample showed the highest ratio. The ratio of the salts in samples was related to the physical properties of the sample and the degree of weathering. Samples of higher densities have more T.D.S ratios than the samples of lower densities. Light yellow samples showed the lowest ratio in T.D.S and densities. The samples of low densities particularly less than 2g/cm^3 having yellow color and consist of the calcite with clay minerals. The clay minerals form more than 30% of the sample so these samples decomposed completely in water in the form of fine grains and characterized with its sticky touch in short time duration. The clay minerals absorb water and changed from state to another according to Atterberg limits and of course the grains of the stone start to decompose and lose its cohesiveness as in table 4.

Table. 3. TDS results of limestone of the mother rock

| Sample | TDS _w | TDS _{w+solid} | TDS _{solid} | TDS % |
|--------------------|------------------|------------------------|----------------------|-------|
| Yellow weak1 | 230 | 1340 | 1110 | 5.55 |
| Yellow weak2 | 230 | 1230 | 1000 | 5.00 |
| Yellow weak 3 | 230 | 1130 | 1100 | 5.50 |
| Average | | | | 5.35 |
| Hard yellow1 | 230 | 1120 | 890 | 4.45 |
| Hard yellow2 | 230 | 1010 | 780 | 3.90 |
| Hard yellow3 | 230 | 1100 | 870 | 4.35 |
| Average | | | | 4.26 |
| Hard light yellow1 | 230 | 1780 | 1550 | 7.75 |
| Hard light yellow2 | 230 | 1660 | 1430 | 7.15 |
| Hard light yellow3 | 230 | 1710 | 1480 | 7.40 |
| Average | | | | 7.43 |

The light-yellow sample of the mother rock appeared no effect on soaking in water and keep in its form and cohesiveness and they recorded higher ratio of T.D.S whereas the salts crystalized on the hard-outer surface in the form of thin layer of fine crust of salts which can be seen under the microscope so the samples recorded the highest ratio of T.D.S. The salts accumulated on the surface and inside cavities and cracks. The white wall sample showed the high ratio of calcite in addition to existence of the dolomite in the XRD and XRF also showed T.D.S values in pillars ranged from 2.0 to 2.3 while in bases decreased to be from 0.49 to 0.51% while in the walls ranged from 0.89 to 1.31%. The temperature degree which measured showed

great variation on the pillars ranged from 29 to 34 and on the walls ranged from 28 to 35 while on the bases ranged from 28 to 33 and thus the values of the surficial moisture showed great variation. The mechanical properties of the white stones recorded higher than 300kg/cm² in the samples so they are suitable for building process according to the Egyptian code for building materials.

Table. 4. TDS results of pillar, bases and white wall

| Sample | TDS _w | TDS _{w+solid} | TDS _{solid} | TDS % |
|---------------|------------------|------------------------|----------------------|-------|
| White pillar1 | 136 | 612 | 476 | 2.38 |
| White pillar2 | 136 | 587 | 451 | 2.26 |
| White pillar3 | 136 | 534 | 398 | 2.00 |
| Average | | | | |
| White wall 1 | 136 | 500 | 364 | 0.98 |
| White wall 2 | 136 | 487 | 351 | 0.93 |
| White wall 3 | 136 | 492 | 356 | 1.31 |
| Average | | | | |
| White base 1 | 136 | 237 | 101 | 0.51 |
| White base2 | 136 | 242 | 106 | 0.52 |
| White base 3 | 136 | 234 | 98 | 0.49 |
| Average | | | | |

Pillars and bases

The results in table 5 showed that, the pillar showed the highest T.D.S values while the bases recorded the lowest T.D.S values. These results showed that, the pillar were the most deteriorated architectural elements while the bases have the lowest deterioration. These results confirmed that the salts were not transported through the bases with the capillary system from ground to base then to the pillar or walls whereas the base was made of special type of limestone with little porosity, water content and high density as we see from the physical properties. As a result, the salts may be transported directly from the debris which accumulated around the elements during existing in the burying environment and then the salts start to crystalize due to the great variation of the temperature and the humidity of the surrounding environment.

Table. 5. Hardness and Compressive strength results of the four walls, columns and bases of Imni Tomb. were between 330-350 kg/cm² and it's a good limestone block for buildings according to Egyptian building materials Code which should be over 250kg/cm²

| eastern wall | northern wall | Western wall | southern wall | column 2 | column 1 | Base 1 | Base2 |
|-------------------------------------|-------------------------------------|-------------------------------------|-------------------------------------|-------------------------------------|-------------------------------------|-------------------------------------|-------------------------------------|
| 36 | 32 | 34 | 34 | 38 | 32 | 19 | 28 |
| 28 | 33 | 32 | 30 | 38 | 32 | 24 | 26 |
| 34 | 30 | 34 | 32 | 34 | 34 | 26 | 26 |
| 30 | 34 | 35 | 34 | 34 | 32 | 30 | 26 |
| 32 | 30 | 35 | 30 | 32 | 32 | 28 | 22 |
| 36 | 34 | 32 | 30 | 32 | 34 | 34 | 20 |
| 35 | 32 | 34 | 30 | 30 | 34 | 34 | 26 |
| 32 | 34 | 30 | 30 | 34 | 34 | 28 | 30 |
| 28 | 36 | 32 | 30 | 32 | 36 | 26 | 30 |
| 34 | 36 | 32 | 30 | 28 | 32 | 26 | 26 |
| R.N=31n/m m ² | R.N=31n/m m ² | R.N=31n/ mm ² | R.N=31n/ mm ² | R.N=35n/m m ² | R.N=33n/m m ² | R.N=22n/m m ² | R.N=18n/m m ² |
| C.S=31*10= 310kg/cm ² | C.S=31*10 =310kg/cm ² | C.S=31*10 =310kg/cm ₂ | C.S=31*10 =310kg/cm ₂ | C.S=31*10 =350kg/cm ₂ | C.S=31*10 =330kg/cm ₂ | C.S=31*10 =220kg/cm ₂ | C.S=31*10 =180kg/cm ₂ |

Compressive Strength

The results in table 5 of compressive strength of pillars and bases ranged from from 330-350kg/cm². They are considered best results. While, the mother rock recorded values from 180-220kg/cm² and this interpreted why the ancient Egyptian preferred to cover the mother rocks with the other type of limestone which brought from out of El-Lishet.

Stone Hardness

The results in table 5 revealed that, hardness of the four walls of Imni tomb was 31, and for the pillars recorded from 33 to 35 and it considers a perfect result but the results of the hardness rate to the mother rock were from 18 to 22 which is considered weak results.

Measurement of Surface Moisture

From table 6, high readings of surface moisture on the southern, northern and eastern walls were observed because they were not exposed to the sun rays, their humidity are relatively high. But readings of the surface moisture which measured for the western wall were low because it was the most walls exposed to the sun rays all the day long. The salts and their appearance on the surface of the western wall are more abundant than those of the other walls. This is because it is drier than the rest of the walls.

Table. 6. Surface moisture results of the mother rock, the four walls, basses and columns of imni tomb

| northern side of the mother rock | western side of the mother rock | southern side of the mother rock | eastern wall of the tomb | northern wall of the tomb | western wall of the tomb** | southern wall of the tomb | base 1 | base 2 | column no.1 | column no.2 |
|----------------------------------|---------------------------------|----------------------------------|--------------------------|---------------------------|----------------------------|---------------------------|--------|--------|-------------|-------------|
| 74 | 87 | 93 | 90 | 89 | 88 | 92 | 88 | 90 | 90 | 88 |
| 75 | 90 | 91 | 91 | 90 | 87 | 92 | 88 | 83 | 89 | 90 |
| 92 | 88 | 97 | 92 | 91 | 88 | 91 | 88 | 87 | 89 | 92 |
| 89 | 85 | 91 | 92 | 90 | 85 | 91 | 88 | 85 | 86 | 90 |
| 87 | 87 | 94 | 88 | 90 | 84 | 93 | 84 | 88 | 87 | 88 |
| 87 | 85 | 92 | 87 | 90 | 88 | 89 | 89 | 82 | 89 | 85 |
| 87 | 97 | 94 | 87 | 89 | 86 | 90 | 90 | 82 | 88 | 85 |
| 88 | 96 | 93 | 92 | 91 | 87 | 88 | 83 | 89 | 87 | 87 |
| 89 | 92 | 93 | 90 | 91 | 88 | 89 | 90 | 84 | 90 | 90 |
| 90 | 91 | 95 | 93 | 88 | 88 | 89 | 85 | 82 | 88 | 83 |
| | | | Sunny | Not sunny | Sunny | Not sunny | 89 | 88 | 89 | 89 |

Temperature measurement

Ambient temperature is equal to 34°C and the relative humidity is 38.7% according to table 7.

Table. 7. Average of Temperature measurement readings results of the Imni tomb walls, and of the tomb columns and bases and the mother rock

| eastern wall of the Tomb | northern wall of the Tomb | western wall of the Tomb | southern wall of the Tomb | northern side mother rock | western side mother rock | southern side mother rock | Bas1 | Bas2 | Colu.1 | Colu.2 |
|--------------------------|---------------------------|--------------------------|---------------------------|---------------------------|--------------------------|---------------------------|------|------|--------|--------|
| 29.0 | 31.3 | 30.0 | 28.0 | 34 | 33 | 28 | 33 | 32.7 | 30 | 30.5 |
| 30.0 | 31.8 | 30.3 | 28.0 | 33 | 31 | 28.8 | 33 | 33 | 31 | 31.6 |
| 30.0 | 30.8 | 30.8 | 27.9 | 34.9 | 32 | 29.1 | 34 | 33 | 30 | 30.9 |
| 30.3 | 31.2 | 30.0 | 28.3 | 33.8 | 34 | 29.3 | 33.8 | 34 | 32.2 | 32 |
| 30.0 | 31.2 | 31.0 | 28.2 | 33.9 | 31 | 28.6 | 30 | 32 | 33.6 | 33 |
| 29.5 | 31.0 | 31.0 | 28.0 | 34 | 33 | 28.8 | 30 | 31 | 31 | 30.7 |
| 29.0 | 31.9 | 31.2 | 27.9 | 35 | 32 | 28 | 31 | 31 | 29 | 31.7 |
| 30.0 | 32.6 | 31.0 | 27.9 | 34 | 33 | 28 | 30 | 32 | 30 | 31.5 |
| 30.0 | 32.5 | 31.5 | 28.1 | 34.7 | 33 | 28.3 | 31 | 33 | 32 | 29 |
| 30.8 | 33.0 | 31.4 | 28.0 | 34.6 | 32 | 28.4 | 28 | 30 | 33 | 29.5 |
| No sun | sun | Sun | No sun | | | | | | | |

The field survey showed that the temperatures of the area before the northern and western wall of Imni tomb were higher than other walls. This is because they expose to the sun rays for longer time than other walls as a result of its location and the sun disc movement during the day time so salt crystallization were noticed much on the western wall of the mother rock in the form of hard crust due to the evaporation process which adapt to the supply of saline solutions. Temperature of columns was higher than their bases because columns expose to the sun rays and air movement all the day long while the bases were covered with layer of sands and dust so the salty crystallization affected badly on the pillars which have cracks and fallen off on the ground.

Discussion

All the previous results showed that the tomb of Imni consisted of two types of limestone; the first is the mother rock where the tomb was hewed and the other type is the white limestone which the pillars and the walls of the tomb were made of. The first type is a local weak type of limestone which contains iron oxides, clay minerals and sodium chloride in the form of halite in addition that it characterized with its great porosity which contributes to transport the saline solutions to crystalize in the form of a thick layer on the exterior surface of the mother rock as a result of evaporation process which happens because of the temperature changes and the wind movement. This crust of salts can be noticed on the western and northern walls which received the most sun rays in the day time and which faces the wind which moves in the direction of northwest. So this crust of salts although it caused fine cracks to the exterior surface of the rocks, it represented a protective layer to this rock wall against weathering process. The salts were transported to the second type of white limestone which was brought from out of El-Lishet and was used in making the walls, pillars and bases of the pillars through diffusion and by capillary system. So the salts in the walls started to crystalize fast below the surface as a result of fast evaporation and slow the supply of saline solutions so the exterior surface of these blocks of stone appeared weak, affected on touching, changing to powder in some cases, small semi separation can be noticed and the weathering increased the bad effects of sub-fflorence. So, the walls lost most of its polished surface and of course the painted inscription.

The pillars of this tomb affected badly; one of them was broken into two parts and salt crust was noticed on the surface of breakage. So it can be interpreted as the pillars was carved from one piece of limestone which was carved versus the sedimentation bedding so the saline solutions which transported through the ground to the pillar crystalized inside between the two layers which form the body of this pillar which was fallen on the ground of the tomb so easily the salts were able to reach and crystalize in the form of layer which in time led to break the pillar into two pieces. The other probability can be interpreted as, on falling of the pillar on the ground, it had fine cracks which the saline solutions invaded and crystalized to break the pillar into two pieces.

Many factors which interact together affect the durability of building materials such as the chemical composition, mechanical resistance environmental conditions as temperature and humidity. Also, type and sources of soluble salts is very important factor. This study was adopted to provide an approach for the salt assessment decay in building material of tomb of Imni and causing salt weathering and the effect of the surrounding conditions prior to examine a suitable treatment procedure for conservation strategies.

Multi analysis methods such as X-ray fluorescence spectrometer, X-ray diffraction spectrometer, optical and polarized microscope, Fourier infra-red spectroscopy and other physical properties measurements as the bulk density, porosity and compressive strength Gave a close picture of the dynamic relationship between the conditions of the tomb stone, the walls, the pillars, and the base and the type of the soluble salt formed, its activity, the surrounding conditions and the deterioration effects. It was proved that, Halite (NaCl) is main soluble salt formed and it was undergoing cycles of recrystallization processes in different places of the

tomb with the impact of the surrounding temperature, humidity and pressure. Also, it was proved that, the salt was transferred from ground to pillars or walls.

Conclusions

As a general conclusion, it can be said that the sodium chloride in the form of halite which was crystalized in different forms and locations was the main cause beyond the deterioration of the exterior polished surfaces of Imni tomb and losing what they had from painted inscription. As a result, many conservation strategies such as protection from water infiltration, reduction of heating temperature and using a kind of inhibitors cause a significant slow-down the crystallization process of the salt.

Acknowledgment

All authors would like to thanks Dr. Moustafa Abdelfatah Restoration director of Giza Mr. Maged Ali Egyptian Ministry of archaeology for all of their supports.

References

- [1] A. Dieter, **Middle Kingdom Tomb Architecture at Lisht**, Vol. 28, Publications of the Metropolitan Museum of Art, Egyptian Expedition, New York, 2008.
- [2] A. Arnold, **Building in Egypt, Pharaonic Stone Masonry**, Oxford University Press, New York, 1991.
- [3] H.C. Hayes, **The Texts in the Mastabeh of Senwosret-ankh at Lisht**, Vol. 12, Publications of the Metropolitan Museum of Art, Egyptian Expedition, New York, 1937.
- [4] W. Toby, **The Rise and Fall of Ancient Egypt**, 2010.
- [5] A. Mace, H. Winlock, **The Tomb of Senebtisi at Lisht**, Vol. 1, Publications of the Metropolitan Museum of Art, Egyptian Expedition, New York, 1953.
- [6] E. Brovanski, *An Inventory List from "Covington's Tomb" and Nomenclature for Furniture in the Old Kingdom*, **Studies in Honor of William Kelly Simpson** (Editor: P. Der Manuelian), Vol. 1, Museum of Fine Arts, Boston, 1996.
- [7] E. Doehne, *Salt Weathering: A Selective Review*, **Geological Society Special Publication Natural Stone, Weathering Phenomena, Conservation Strategies and Case Studies**, **205(1)**, 2002, pp. 51-64.
- [8] A. Arnold, K. Zehnder, *Decay of stony materials by salts in humid atmosphere*. In: J. Ciabach (Editor), **Proceedings of the 6th International Congress on Deterioration and Conservation of Stone**, Nicholas Copernicus University, Torun, Poland, 1988, pp. 138-148.
- [9] A. Arnold, K. Zehnder, *Monitoring wall paintings affected by soluble salts*, **The Conservation of Wall Paintings, Proceedings of a Symposium organized by The Courtauld Institute of Art and the Getty Conservation Institute**, London, July 13-16, 1987, Getty Conservation Institute, Marina del Rey, 1991, pp. 103-135.
- [10] M. El-Gohary, *Investigation on Limestone weathering of El Tuba Minaret El Mehalla, Egypt, A case study*, **Mediterranean Archaeology and Archaeometry**, **10(1)**, 2010, pp. 61-79.
- [11] A.E. Charola, *Salts in the deterioration of porous materials: An overview*, **Journal of the American Institute for Conservation**, **39(3)**, 2000, pp. 327-343. <https://doi.org/10.1179/019713600806113176>
- [12] L. Dei, M. Mauro, P. Baglioni, C. Manganelli Del Fà, F. Fratini, *Growth of crystal phases in porous media*, **Langmuir**, **15(26)**, 1999, pp. 8915-8922.
- [13] S. Brüggerhoff, P.W. Mirwald, *Examination of complex weathering processes on different stone materials by field exposure studies*, **7th International Congress on Deterioration and Conservation of Stone** (Editors: D. Rodrigues, F. Henriques, and F.T. Jeremias), **Lisbon, 1991, pp. 715 - 724**.

- [14] C. Bohm, A. Kong, K. Zehnder, *Salt Crystal Intergrowth in Efflorescence on Historic Buildings*, Art and Chemical Sciences, **Chimia**, **55**(11), 2001, pp. 996-1001.
- [15] M. Steiger, *Salts in porous materials: Thermodynamics of phase transitions, modeling and preventive conservation*, **Restoration of Buildings and Monuments**, **11**, 2005, pp.419–431.
- [16] A.M.A. Moussa, N. Kantiranis, K.S. Voudouris, J.A. Stratis, M.F. Ali, V. Christaras, *The Impact of soluble salt on the deterioration of pharaonic and Coptic wall paintings at al qurna, Egypt: Mineralogy and Chemistry*, **Archaeometry**, **51**(2), 2009, pp. 292-308. <https://doi.org/10.1111/j.1475-4754.2008.00422.x>
- [17] S. Abdelaal, I.C.A. Sandu, *Assessment of protease in cleaning of bat blood patches from ancient Egyptian wall paintings and surface inscriptions*, **International Journal of Conservation Science**, **10**(3), 2019, pp. 459-474.
- [18] R. Flatt, *Salt damage in porous materials: How high supersaturations are generated*, **Journal of Crystal Growth**, **242**(3), 2002, pp. 435-454. DOI: 10.1016/S0022-0248(02)01429-X
- [19] A. Arnold, K. Zehnder, *Crystallization and habits of salt efflorescences on walls. I - Methods of investigation and habits*. In: Félix, G. (editor) **Proceedings of the 5th International Congress on the Deterioration and Conservation of Stone**, Lausanne, Presses Polytechniques Romandes, 1985, pp. 255–267.
- [20] A. Arnold, K. Zehnder, *Crystallization and habits of salt efflorescences on walls II. Conditions of crystallization*. In: Félix, G. (ed.), **Proceedings of the 5th International Congress on the Deterioration and Conservation of Stone**, Lausanne, Presses Polytechniques Romandes, 1985, pp. 269–277.
- [21] T.D. Gonçalves, *Salt crystallization in plastered or rendered walls*, **PhD Thesis**, Universidade Tecnica Lisboa, Instituto Superior Tecnico, Lisbon, 2007.
- [22] M. Pirak, *Analysis of Erosion Caused by Soluble Salts in Historical Monuments*, **Journal of research on Archaeometry**, **1**(2), 2016, pp. 51-73. DOI: 10.29252/jra.1.2.51.
- [23] G. Ahmad, F. Abdul Rahman, *Treatment of salt attack and rising damp in heritage buildings in Penang, Malaysia*, **Journal of Construction in Developing Countries**, **15**(1), 2010, pp. 93-113.
- [24] A. Urland, E. Borrelli, **Salts. ICCROM ARC Laboratory Handbook** (Conservation of architectural heritage, historic structures and materials). ICCROM, Roma, 1999.
- [25] N. ČukovskaI, G. Orhideja, *Characterization of salt efflorescence using target factor analysis. Development of the method*, **Journal of the Brazilian Chemical Society** (São Paulo), **20**(1), 2009, pp. 57-63. <http://dx.doi.org/10.1590/S0103-50532009000100011>
- [26] J. Hradilova, T. Grygar, S. Švarcová, P. Bezdička, E. Kočí, *Degradation of lead-based pigments by salt solutions*, **Journal of Cultural Heritage**, **10**(3), 2009, pp. 367–378.
- [27] S. Abdelaal., *New Approach of Characterization and State of Painted Reliefs in Petosiris Tomb, Tuna El-Gebel, Egypt*, **International Journal of Conservation Science**, **9**(4), 2018.
- [28] S. Abdelaal, *New Approach for study of wall paintings in Abuellleaf monastery, Fayoum oases, Egypt*, **International Journal of Conservation Science**, **9**(3), 2018, pp. 709-722.
- [29] M. Abdelfatah, M. Kallaaf, H. Immam, S. Abdelaal, *The Role of Geotechnical Properties of Rocks in Failure of Stability of the Funeral Subsurface Structure in Saqqara Plateau, Egypt: Part I*, **The Journal of Center for the Global Study of Cultural Heritage and Culture**, **5**, 2017.
- [30] D. El Sherbiny, N. Ali, S. Abd El Aal, J. Vallet, *A multi-analytical approach applied to the archaeometric study of a greco-roman decorated wooden panel from Egypt*, **Journal of Ancient Egyptian Interconnections**, **7**(4), 2015, pp. 27-37.
- [31] S. Abdelaal, J. Vallet, J. Berthonneau, G. Mhagoub, E. Ali, *Degradation of Engraved Stone and Renders from Qasr Qarun Temple in Fayoum Oasis, Egypt*, **Proceedings of the International Conference on Conservation of Stone and Earthen Architectural Heritage**, The Graduate School of Cultural Heritage Kongju National University, Republic of Korea, ICOMOS-ISCS International Conference, 2014, pp. 171-180.

- [32] S. Abdelaal, M. Ali, A. Turos, A. Korman, A. Stonert, *PIXE Analysis of Ancient Egyptian Pigments. Case Study*, **Journal of Nano Research**, **8**, 2009, pp. 71-77.
- [33] S. Abdelaal, M. Ali, G. Mahgoub, S. Abdeleazeim, A. Turos, A. Stonnert, *The Use of Analytical Methods in Evaluation of Coptic Wall Paintings Conservation A Case Study*, **Acta Physica Polonica A**, **120**(1), 2011, pp. 120-144.
- [34] S. Abd El Aal, *Identification of Painting Layers of Sennefer Tomb by Ion Beam Analysis*, **Acta Physica Polonica A**, **120**(1), 2011, pp. 144-148.
- [35] S. Abd El Aal, A Korman, A. Stonert, F. Munnik, A. Turos, *Ion beam analysis of ancient Egyptian wall paintings*, **Vacuum**, **83**(Suppliment 1), 2009, pp. S4-S8. <https://doi.org/10.1016/j.vacuum.2009.01.012>
- [36] E. Polychroniadou, *Optical and analytical techniques applied to the Amfissa Cathedral mural paintings made by the Greek artist Spyros Papaloukas (1892-1957)*, **Revue d'Archaeometrie (Archaeosciences)**, **31**, 2007, pp. 97-112.
- [37] E. Osmani, Y. Zidan, N. Kamal, *Using the Microscopic and Spectroscopic Techniques to Identify and Characterize Archaeological Artifacts*, **International Journal of Conservation Science**, **5**(4), 2014, pp. 459-468.
- [38] S. Abdelaal, N. Mahmoud, V. Detalle, *A technical examination and the identification of the wood, pigments, ground and Binder of an ancient Egyptian Sarcophagus*, **International Journal of Conservation Science**, **5**(2), 2014, pp. 177-188.
- [39] D. Andrews, *Optical Techniques for the Analysis and Characterization of Chemicals and Materials*, **digital Encyclopedia of Applied Physics**, 2005, pp.23-56
- [40] G. Rahman, B. Abdul, *Scanning Electron Microscopy in Archaeology: The Analysis of Unknown Specimen Recovered from District Shangla, Pakistan*, **Journal of Asian Civilizations (Islamabad)**, **38**(1), 2015, pp. 153-167.
- [41] S.H. Kuckova, M.C. Krizkova, C.L.C. Pereira, R. Hynek, O. Lavrova, T. Busani, L.C. Branco, I.C.A. Sandu, *Assessment of Green Cleaning Effectiveness on Polychrome Surfaces by MALDI-TOF Mass Spectrometry and Microscopic Imaging*, **Microscopy Research and Technique**, **77**(8), 20145, pp. 574-585. DOI: 10.1002/jemt.22376
- [42] S. Prati, E. Joseph, G. Sciutto, R. Mazzeo, *New Advances in the Application of FTIR Microscopy and Spectroscopy for the Characterization of Artistic Materials*, **Accounts of Chemical Research**, **43**(6), 2010, pp. 792–801. doi: 10.1021/ar900274f.
- [43] S.-C. Litescu, E.D. Teodor, G.-I. Truica, A. Tache, G.-L. Radu, *Fourier Transform Infrared Spectroscopy Useful Analytical Tool for Non-Destructive Analysis (Chapter 13) Infrared Spectroscopy - Materials Science, Engineering and Technology* (Editor: T. Theophanides), InTech, 2012, pp. 353-363.
- [44] G. Shearer, *An Evaluation of Fourier Transform Infrared Spectroscopy for the Characterization of organic Compounds in art and Archaeology*, **PhD Thesis**, (Thesis of Doctor of Philosophy), Faculty of Science, University College London, 1989, 399p.
- [45] Z. Glavcheva, D. Yancheva, Y. Kancheva, E. Velcheva, B. Stamboliyska, *Development of FTIR spectra database of reference art and archaeological materials*, **Bulgarian Chemical Communications**, **46**, A, 2014, pp. 164 – 169
- [46] M. Baker, C. Hughes, K. Hollywood, *Vibrational Spectroscopic Diagnostics*, **Infrared Spectroscopy**, 2016 Morgan & Claypool Publishers, pp. 2-14
- [47] J. Font, S. Salvadó, S. Buti, J. Enrich, *Fourier transform infrared spectroscopy as a suitable technique in the study of the materials used in waterproofing of archaeological amphorae*, **Analytica Chimica Acta**, **598**(1), 2007, pp. 119-127. DOI: 10.1016/j.aca.2007.07.021
- [48] B. Stuart, *Infrared Spectroscopy: Fundamentals and Applications*, **Analytical Techniques in the Sciences**, John Wiley & Sons, Ltd., 2004, 231p.
- [49] S. Palanivel, S. Meyvel, *Microstructure and Microanalytical Study – SEM of Archaeological Pottery Artifacts*, **Romanian Journal of Physics**, **55**(3-4), 2010, pp. 333–341.

- [50] J.J. Ojeda, M. Dittrich, *Fourier Transform Infrared Spectroscopy for Molecular Analysis of Microbial Cells*, **Method in Molecular Biology**, **881**, 2012, pp 187-211. doi: 10.1007/978-1-61779-827-6_8.
- [51] E. Franceschi, *X-Ray Diffraction in Cultural Heritage and Archaeology Studies*, **Open Access Library Journal**, **1**, 2014, pp. 1-10.
- [52] M. Schreiner, B. Frühmann, D. Jembrih-Simbürger, R. Linke, *X-rays in art and Archaeology - An over view*. **Advanced in X-ray analysis** (International center for diffraction data), **47**, 2004, pp. 1-18.
- [53] M. Uda, G. Demortier, I. Nakai, **X-rays for Archaeology**, Springer, Netherlands, 2005.
- [54] I.C.A. Sandu, E. Murta, S. Ferreira, M.F.C. Pereira, S.H. Kuckova, V. Valbi, L. Dias, C. Prazeres, A.M. Cardoso, J. Mirao, A.E.G. Candeias, *A Comparative Multi-Technique Investigation on Material Identification of Gilding Layers and the Conservation State of 7 Portuguese Mannerist Altarpieces*, **International Journal of Conservation Science**, **6**, 2015, pp. 439-454 Special Issue: SI.
- [55] I.C. Frestone, A.P. Middleton, *Mineralogical applications of the analytical SEM in archaeology*, **Mineralogical Magazine**, **51**(359), 1987, pp. 21-31. DOI: <https://doi.org/10.1180/minmag.1987.051.359.03>
- [56] I. Sandu, O. Mircea, A.V. Sandu, I. Sarghie, I.G. Sandu, V. Vasilache, *Non-invasive Techniques in the Analysis of Corrosion Crusts Formed on Archaeological Metal Objects*, **Revista de Chimie**, **61**(11), 2010, pp. 1054-1058.
- [57] A.D. Hill, A.H. Lehman, M.L. Parr, *Using Scanning Electron Microscopy with Energy Dispersive X-ray Spectroscopy To Analyze Archaeological Materials. Introducing Scientific Concepts and Scientific Literacy to Students from All Disciplines*, **Journal of Chemical Education**, **84**(5), 2007, p. 810. <https://doi.org/10.1021/ed084p810>
- [58] J. Dezuane, **Handbook of Drinking Water Quality**, 2 ed, John Wiley & Sons, 1997.
- [59] C. Sawyer, P. McCarty, **Chemistry for Sanitary Engineers**, 2nd ed., McGraw-Hill Series in Sanitary Science and Water Resources Engineering, Mc Graw Hill, New York, 1967.
- [60] M. Abdelaziz, **Total Dissolved Solids in Drinking-Water, Guidelines for Drinking-Water Quality**, 2nd ed., Vol. 2, Health Criteria and Other Supporting Information. World Health Organization, Geneva, 1996.
- [61] T. Singh, Y.P. Kalra, *Specific conductance method for in situ estimation of total dissolved solids*, **Journal of the American Water Works Association**, **67**(2), 1975, pp. 99-100. <https://doi.org/10.1002/j.1551-8833.1975.tb02168.x>
- [62] V. Stremah, *Estimation of damage at the surface of stones using nondestructive techniques*, **5th International Congress Structural Studies, Repairs and Maintaince of Historical Buildings**, San Sebastian, Advances in Architectural Series of Computetional Mechanics Publications, Southampton, 1997, pp. 121-128.
- [63] J. Cassar, M. Winter, B. Marker, N. Walton, D. Entwisle, **Stone in Historic Buildings: Characterization and Performance**, Geological Society, London, Special Publications, 391, 2014.
- [64] S. Siegesmund, T. Weiss, *Natural Stone, Weathering Phenomena, Conservation Strategies and Case Studies*, Geological Society, London, Special Publications, 205, 2002, pp. 1-7.
- [65] M. Balintova, A. Estokova, *Analysis of Building Stone of the Medieval Historical Building*, **Advanced Materials Research**, **897**, 2014, pp. 305-308.

Received: February 20, 2019

Accepted: August 30, 2019